ORIGINAL RESEARCH Open access

A Flight Speed-Aware Vehicle Routing Problem for Drone Delivery under Load and Wind Conditions

Emily Johnson[1*], Robert Smith[1], Laura Brown[2], Kevin Miller[3], David Thompson[4]

Abstract

Delivery drones have emerged as a highly promising solution for package transportation, drawing considerable interest from both industry and academia. Several studies on routing optimization designed specifically for drone-based delivery have extended classical Vehicle Routing Problems (VRPs). While most traditional VRPs draw on Traveling Salesman Problems (TSPs) to minimize total travel distance, drone-oriented VRPs place greater emphasis on energy consumption due to strict battery limitations. Although the energy required for hovering with loaded packages accounts for a substantial share of total consumption—since drones must remain airborne while carrying multiple items—only limited research has focused on drone routing models to minimize total flight duration. Furthermore, flight duration is significantly impacted by wind patterns such as headwinds and tailwinds. This paper introduces a new VRP variant for drone delivery, in which flight time varies with package weight under windy conditions, referred to as the Flight Speed-aware Vehicle Routing Problem with Load and Wind (FSVRPLW). Within this framework, flight speed is dynamically adjusted based on both payload and wind direction. In particular, heavier loads reduce flight speed, whereas lighter loads allow higher speeds. Similarly, headwinds reduce speed, while tailwinds enhance it. We provide a mathematical formulation of the problem and introduce a dynamic programming algorithm for its solution. An experimental analysis examines the extent to which package weight and wind conditions affect overall flight time. Results show that incorporating both load and wind factors is highly effective for reducing flight duration. Additionally, comparative assessment indicates that package weight exerts a stronger influence on flight time than wind conditions.

Keywords Drone, Drone routing problem, Flight speed-aware vehicle routing problem, Dynamic programming algorithm

*Correspondence:
Emily Johnson
emily.johnson@utoronto.ca
[1] Department of AI for Smart Grain Bin Monitoring and Aeration Control, Faculty of Agriculture, University of Toronto, Toronto, Canada
[2] Department of Machine Learning for Mycotoxin Risk Prediction, Faculty of Agriculture, McGill University, Montreal, Canada
[3] Department of Precision Harvest Logistics, Faculty of Agriculture, University of Guelph, Guelph, Canada
[4] Department of Smart Dryer Temperature Optimization, Faculty of Agriculture, University of Saskatchewan, Saskatoon, Canada

Introduction

Over the past few years, drones have shown strong potential for diverse practical applications. Their ease of use has led to widespread adoption in recreational activities and content creation. Notably, utilizing drones for last-mile package delivery stands out as a particularly valuable application. Compared to conventional ground-based delivery systems, drone delivery provides multiple key benefits. Operating through the air enables drones to bypass road congestion and surface obstacles entirely. Operating on electricity, they generate reduced CO2 emissions, and the absence of onboard pilots contributes to lower operational labor expenses. Kirschstein [1] analyzed the energy efficiency advantages of delivery drones and concluded that they outperform traditional truck deliveries. Because drones require no human

This is an open access article distributed under the terms of the Creative Commons Attribution-NonCommercial-ShareAlike 4.0 International License (CC BY-NC-SA 4.0), which permits non-commercial use, distribution, reproduction, and adaptation in any medium or format, provided that appropriate credit is given to the original author(s) and source, a link to the license is provided, and any changes made are indicated. Adapted material must be distributed under the same license.

© 2026 The Author(s). | Published by Agro Intelligence Research Press

operator, they inherently reduce staffing costs relative to manned vehicle deliveries. Several organizations have already begun implementing drone logistics services [2, 3]. As a result, research into efficient route planning for drone delivery has intensified substantially over the last ten years [4-7].

The foundation of drone package delivery dates back to the Traveling Salesman Problem (TSP) [8]. Vehicle Routing Problems (VRPs) emerged as a significant extension to better reflect realistic vehicle constraints. Classical VRPs were primarily designed for ground trucks, meaning they did not incorporate drone-specific operational traits. Dorling *et al.* [9] were among the first to examine routing challenges tailored to drones. Since then, numerous VRP extensions customized for drone delivery have been proposed. A large portion of this research has centered on energy management, as battery-powered drones typically have restricted endurance. However, most proposed energy consumption models are limited to specific drone models, restricting their general applicability. From an energy standpoint, total flight time—comprising both hovering and transit phases—represents a vital consideration, as maintaining hover while carrying cargo consumes considerable power [10]. Despite this reality, most existing drone delivery models have relied on the assumption of constant flight velocity. In actual operations, drones must transport varying loads and adjust their speed accordingly. Funabashi *et al.* [11] developed a planning method that accounts for speed variations caused by different package weights. In addition, environmental factors such as wind play a major role. Tailwinds accelerate movement, whereas headwinds impede progress. Ito *et al.* [12], Luo *et al.* [13], and Guerrero and Bestaoui [14] developed wind-aware VRPs for drones. However, these works did not integrate the simultaneous impact of package weight on flight performance.

This paper presents a novel VRP for drone delivery that accounts for the combined effects of package weight and wind on flight speed, explicitly minimizing total flight time. Typical drone operations range from 0 to 23 m/s and support payloads up to 25 kg [15], with capacity varying by drone model. The current work extends the earlier study [11] by addressing additional factors. While Ref. [11] focused solely on load-induced speed changes, wind conditions are equally critical for determining optimal delivery sequences. The proposed model, Flight Speed-aware Vehicle Routing Problem with Load and Wind (FSVRPLW), jointly considers both elements to better capture the dominant contributors to flight duration. Conventional approaches treat drone speed as fixed, yet real-world conditions cause speed to fluctuate with payload mass and wind. To address this gap, we define a new variant of the problem. Here, flight speed decreases under heavy loads and increases under light loads. Likewise, headwinds slow the drone, and tailwinds accelerate it. We derive a formal mathematical model for FSVRPLW and design a dynamic programming algorithm to solve it. Scalability is also tested by measuring computation time across varying numbers of delivery points. Given packages for delivery and prevailing wind data, FSVRPLW identifies the optimal tour that starts and ends at the depot, delivers to all customers, and accounts for wind effects. The developed dynamic programming method efficiently computes the minimal-time route.

The remainder of this paper is structured as follows. Section 2 reviews related work. Section 3 presents the FSVRPLW for delivery drones. Section 4 introduces a dynamic programming algorithm for FSVRPLW. Section 5 discusses the evaluation; finally, Section 6 concludes the paper.

Related Works

Lately, various strategies for drone-based package delivery have been the subject of detailed review [4-7]. Route optimization for drones has mainly been explored through extensions of TSPs [16-20]. Agatz *et al.* [16] developed a flying sidekick model that arranges delivery sequences combining drones with trucks. Bouman *et al.* [17] offered a dynamic programming technique for coordinating deliveries shared between trucks and drones. Works from [16, 17] ignore any idle periods following completion of each drop-off by either vehicle. Marinelli *et al.* [18] and Ha *et al.* [19] designed approaches to reduce waiting times for both trucks and drones and to lower drone power consumption. Murray and Chu [20] outlined a setup assuming drones launch directly from trucks. Tu *et al.* [21], Kitjacharoenchai *et al.* [22], Saleu *et al.* [23], and Ham [24] broadened the framework to involve several drones operating alongside trucks. Ham [24] handled cases where drones manage package retrieval in addition to drops. Although earlier efforts mostly limited drones and trucks to single tasks per outing, Ham [24] included retrieval actions. Still, the bulk of these efforts rests on basic routing

© 2026 The Author(s). | Published by Agro Intelligence Research Press

premises. Put differently, models rooted in TSPs overlook distinctive vehicle features. For drones in particular, speeds and durations can shift dramatically with payload mass, power levels, and surrounding conditions. Thus, TSP-style routing falls short when seeking workable paths.

Building further on TSPs, VRP-style models that integrate vehicle traits have arisen to deliver more realistic solutions. In contrast to TSPs, VRPs target reductions in power use, completion times, and covered distances by weighing vehicle-specific factors. For drones, reducing the full operational expense of aerial trips is especially vital. Multiple investigations weigh delivery expenses across truck-drone combinations, as seen in Poikonen *et al.* [25], Wang *et al.* [26], and Ha *et al.* [27].

Avoiding malfunctions makes energy reduction the central target in drone operations. As a result, Energy Minimizing Vehicle Routing Problems (EMVRPs) were introduced by Ito *et al.* [12], Kara *et al.* [28], and Funabashi *et al.* [29]. Drone power draw is usually determined by prolonged hovering. Confirmation comes from Refs. [10] and [30], which report tests on an AR Drone 2.0 at various velocities and cargo masses. Those trials kept speeds below 6 m/s and loads below 168 g. Outcomes confirm that load mass alters speed, which, in turn, heavily affects power requirements. From here, models featuring adjustable velocities and durations have surfaced. Dorling *et al.* [9] outlined a scheme that weighed load masses and battery states by their influence on power and duration. By comparison, Poikonen *et al.* [25], Wang *et al.* [26], and Ha *et al.* [27] fixed speeds regardless of carried items. Separately, the Flight Speed-aware Vehicle Routing Problem (FSVRP) — which adjusts speeds per load — was introduced in Ref. [11]. Reference [11] factors in velocity shifts from cargo. To be exact, larger loads slow the drone, but smaller ones allow faster travel. The assumption held the lift force constant, tying speed directly to the carried mass. Shorter overall duration than trims total power draw. Funabashi *et al.* [11] indeed achieved lower consumption levels. Sadly, actual speeds are disrupted by wind and loads. Few studies have examined the effects of wind on drone velocity [12-14]. Funabashi *et al.* [11], Ito *et al.* [12], and Bouman *et al.* [17] crafted swift dynamic programming solvers for these routing tasks. Genetic algorithms have also served as effective optimizers. A range of papers harness genetic algorithms — an AI technique — for planning drone routes [27, 31, 32]. Even so, combined attention to both load and wind in delivery routing remains absent. As far as we know, the present effort marks the first examination of how load and wind together shape total flight duration.

A Description of FSVRPLW

The suggested model builds on the FSVRP model originally proposed by Funabashi *et al.* [11]. Unlike FSVRP, it merges load mass with wind effects; hence the name Flight Speed-aware Vehicle Routing Problem with Load and Wind (FSVRPLW). Upcoming sections supply a motivating case to underline its value and lay out the formal math.

A motivational example

Figure 1 depicts a sample instance of the discussed issue. It maps customer separations alongside delivery package masses for a three-customer scenario. Weights use g units, while wind moves constantly at 2 m/s along one fixed bearing. Drone base velocity stands at 5 m/s.

© 2026 The Author(s). | Published by Agro Intelligence Research Press

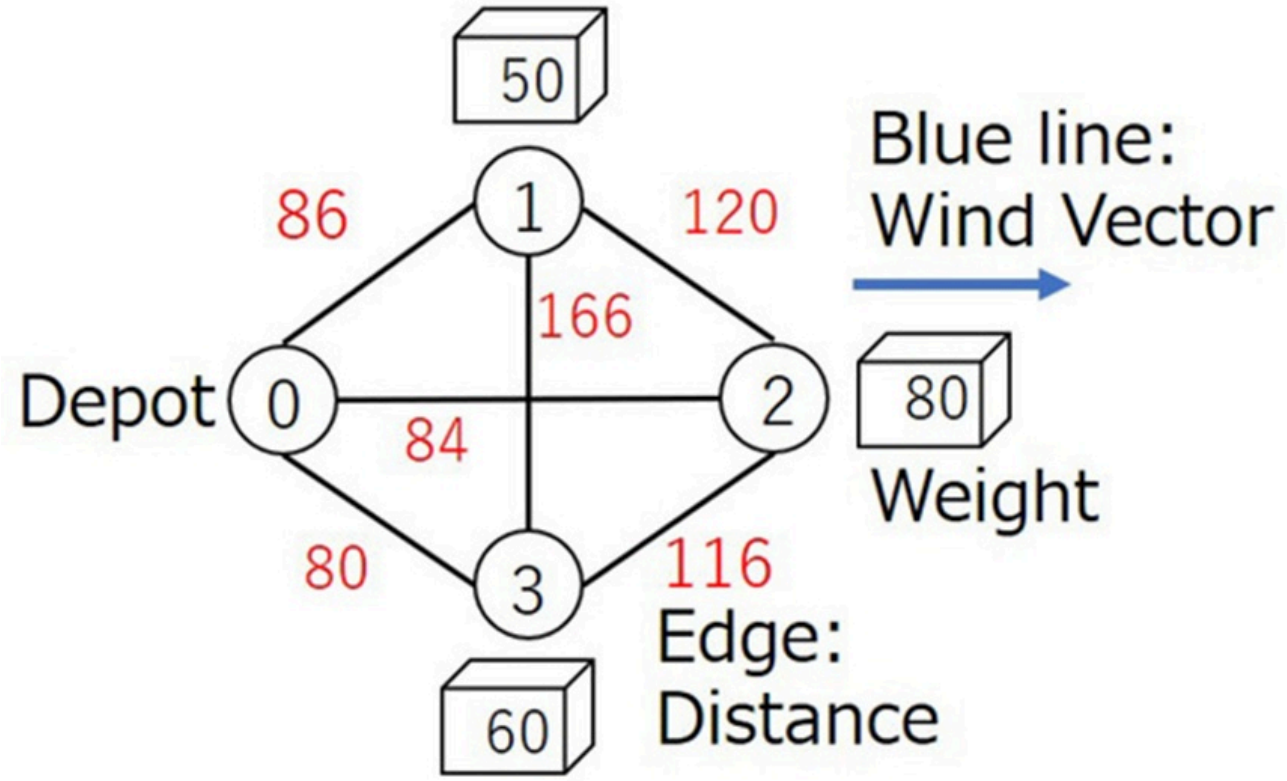


Figure 1. An example problem.

Nodes mark customers, connecting lines show travel spans, and boxed areas list package masses per stop. Node 0 stands for the depot. For example, moving from depot to customer 2 involves carrying an 80 g item over 84 distance units. Observe that the wind flows from the depot toward customer 2.

FSVRP alters velocity per load mass. Substantial masses cut speed; modest masses raise it. Given this property, early handling of heavy items appears sensible for trimming the full duration. Nevertheless, wind forces can impede motion and require attention.

Figures 2a and 2c present the best route for FSVRP. **Figure 2a** covers distances under FSVRP, while **Figure 2c** lists durations. **Figures 2b and 2d** cover the best route for FSVRPLW. **Figure 2b** covers distances under FSVRPLW, while **Figure 2d** lists durations. Durations here adjust for load and wind shifts. Full computation steps are covered in Sections 3.2 and 3.3. Across **Figures 2a–2d**, red paths mark the sequence cutting total duration in FSVRP. Drone duration is determined by the cumulative span and load masses.

© 2026 The Author(s). | Published by Agro Intelligence Research Press

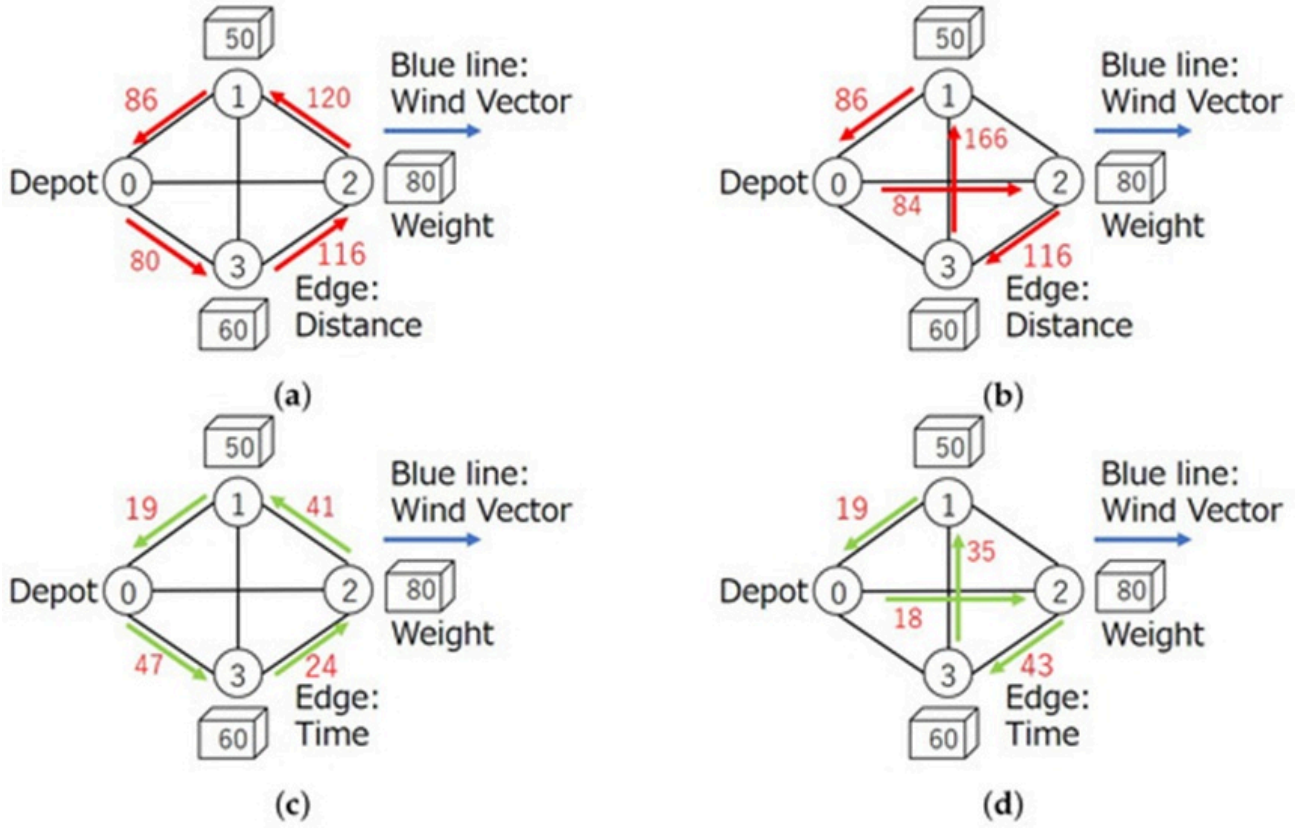


Figure 2. Comparison of FSVRP and FSVRPLW: (a) flight distance of FSVRP, (b) flight distance of FSVRPLW, (c) flight time of FSVRP, and (d) flight time of FSVRPLW.

Keep in mind that heavier masses reduce velocity and stretch durations. This points toward early heavy deliveries. Yet the genuine best answer diverges from that view, since distance also weighs heavily when shortening times. For the FSVRP case, cumulative distance totals 402 (= 80 + 116 + 120 + 86), and duration totals 131 (= 47 + 24 + 41 + 19). FSVRPLW layers wind into route selection. Its best path shows in **Figures 2b and 2d**. Here, supportive tailwind between depot and customer 2 boosts motion, placing customer 2 first. Accordingly, cumulative distance under FSVRPLW hits 452 (= 84 + 116 + 166 + 86), and duration reaches 115 (= 18 + 43 + 35 + 19).

The sample shows that drones follow distinct trajectories between FSVRP and FSVRPLW. FSVRP tends to serve heavy-mass, nearby customers initially. Thus, customer 3 comes first thanks to its mass and brief span. Meanwhile, FSVRPLW trims overall duration via helpful winds. In this instance, the bulkiest item is sent to customer 2 first, enabling swift progress despite greater separation. Under FSVRPLW, duration drops even across extended paths.

FSVRPLW formulation

This section details the setups for FSVRP and FSVRPLW.

N packages await delivery. For broad applicability, at most two packages target any one customer, yielding N total customers. Packages bound for identical stops merge upfront. Packages here cover one outing, eliminating duplicate tours. Extra stops at a single customer during a single outing waste power and time. Customer i ($1 \leq i \leq N$) receives package i; depot holds number 0 per **Figure 1**. All items load at the outset from the depot. Excess total mass beyond drone limits would require additional runs, but that would exceed current coverage. Let (i1,2) mark the span from customer i1 to i2. Let (j) name the j-th stop, acting as a routing choice. Routes open and close at the depot, so we set forth the next definitions.

© 2026 The Author(s). | Published by Agro Intelligence Research Press

$$x(0) = x(N+1) = 0 \quad (1)$$

Further, each customer receives one visit, stated formally below.

$$1 \le x(j) \le N \qquad (1 \le j \le N) \quad (2)$$

$$x(j_1) \ne x(j_2) \qquad (1 \le j_1, j_2 \le N, j_1 \ne j_2) \quad (3)$$

Let (i) mark the mass of package i, and Wd the drone base mass. Let (j) show the full carried mass leaving the j-th customer. Full load exists at the depot exit. Hence, the equation applies.

$$W(0) = \sum_{i=1}^{N} w(i) \quad (4)$$

At the j-th halt ($1 \le j \le N$) with customer (j), mass ((j)) leaves. So, carried mass after exit from customer (j) equals:

$$W(j) = W(j-1) - w(x(j)) \quad (5)$$

Let (i1,2) mark the duration from customer i1 to i2. Time from i1 to i2 equals the span split by present velocity. With vl load-dependent, the time from the j-th to (j+1)-th equals:

$$t(x(j), x(j+1)) = d(x(j), x(j+1)) / v_l(W(j)) \quad (6)$$

FSVRP hunts the lowest duration among routes, the objective given by:

$$\textbf{minimize} \qquad T = \sum_{j=0}^{N} d(x(j), x(j+1)) / v_l(W(j)) \quad (7)$$

FSVRPLW here receives a formal statement thus. Given w, d, and v, locate x minimizing objective (7) under constraints (1)–(6).

FSVRPLW folds wind into FSVRP velocity. Let vlw equal the velocity blending wind with load. vlw varies by mass, wind velocity, and customer position vector. With drone velocity vlw, wind velocity vw, and vector ((j),(j+1)) linking (j) to x(j+1), **Eq. 6** reads:

$$t(x(j), x(j+1)) = \frac{|\mathbf{c}(x(j), x(j+1))|}{v_{lw}(W(j), v_w, \mathbf{c}(x(j), x(j+1)))} \quad (8)$$

Hence, FSVRPLW hunts the lowest duration among routes, the objective given by:

© 2026 The Author(s). | Published by Agro Intelligence Research Press

$$\textbf{minimize} \quad T = \sum_{j=0}^{N} \frac{|c(x(j), x(j+1))|}{v_{lw}\left(W(j), v_w, c\left(x(j), x(j+1)\right)\right)} \tag{9}$$

The FSVRPLW addressed in this paper is formally defined as follows. Given w, v, vw, c, and vlw, find x, which minimizes the objective function (9) while meeting constraints (1)–(5), (8).

Effects on flight speed of a drone

The drone flight speed function vlw introduced in the earlier section depends on the specific drone type. For this research, vlw is treated as an input value, and an illustration of its computation appears in the following. We begin by examining how payload influences drone velocity.

Figures 3a and 3b demonstrate the effects of payload on movement speed. The diagrams present lateral views of the drone. **Figure 3a** corresponds to the no-payload scenario. Here, P denotes lift force while θ stands for pitch angle. Furthermore, Wd signifies the drone's inherent mass. To prevent descent, the upright element of P (called Py) must match the gravitational pull $Wd{\cdot}g$. θ indicates the pitch setting where Py counters gravity exactly.

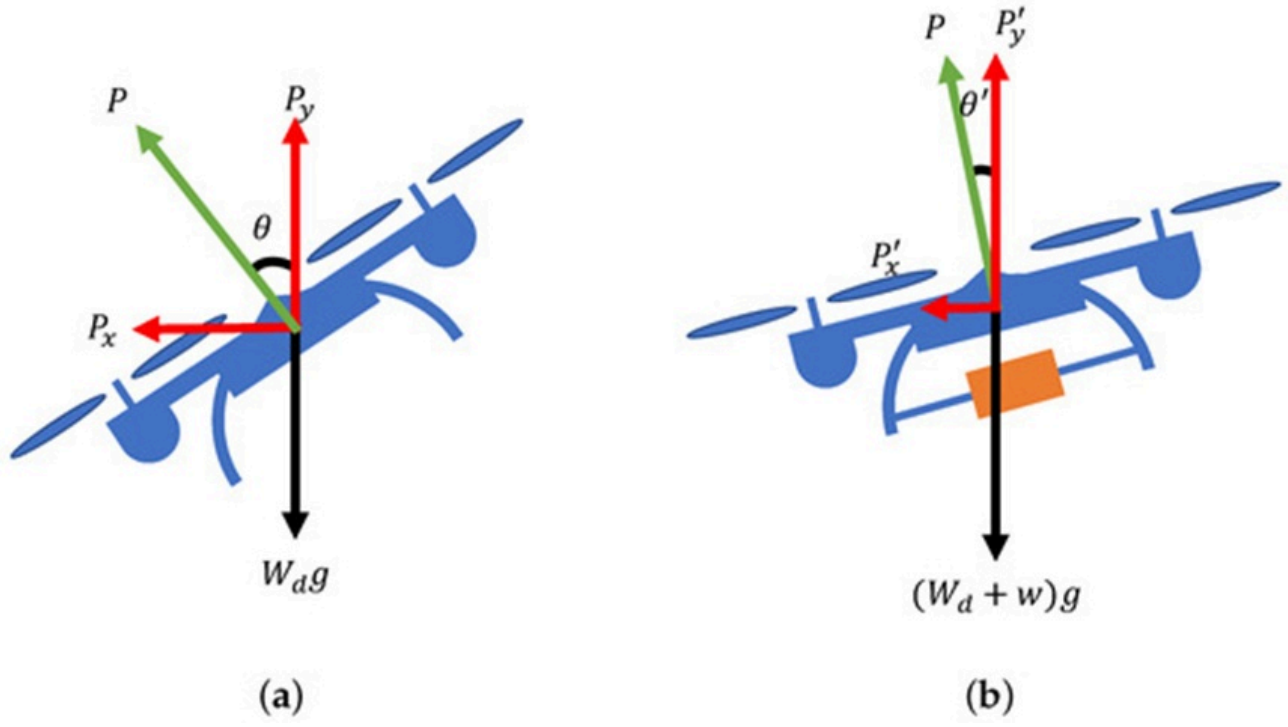


Figure 3. Effect of load: (a) drone without load and (b) drone with load w.

P's sideways element (Px) supplies propulsion toward the target and matches air drag $k{\cdot}(0)$, where k serves as a model-specific constant.

$$P_x = P \sin(\theta) = k \cdot v_l(0) \tag{10}$$

Figure 3b portrays the drone in motion bearing load w. Maintaining altitude requires pitch angle θ' to stay under θ. This produces the relations below.

© 2026 The Author(s). | Published by Agro Intelligence Research Press

$$P'_y = P \cos(\theta') = (W_d + w) \cdot g \quad (11)$$

$$P'_x = P \sin(\theta') = k \cdot v_l(w) \quad (12)$$

Hence, we derive the following.

$$v_l(w) = \frac{P}{k} \sin(\theta') = \frac{\sin(\theta')}{\sin(\theta)} v_l(0) \quad (13)$$

$$\theta' = \arccos\left(\frac{(W_d + w) \cdot g}{P}\right) \quad (14)$$

$$\theta = \arccos\left(\frac{W_d \cdot g}{P}\right) \quad (15)$$

Therefore, the drone's flight speed when loaded is as follows.

$$v_l(w) = \frac{P}{k} \sin\left(\arccos\frac{(W_d + w) \cdot g}{P}\right) \quad (16)$$

Attention now turns to wind acting along the drone's path. When the wind opposes progress, drone velocity decreases due to the wind's push. In short, wind velocity subtracts from overall speed. Yet wind may also accelerate motion. When blowing along the travel path, the wind adds to the drone's velocity. External wind produces major shifts in drone pace. Wind velocity here remains below the drone's peak calm-air speed. This avoids situations where targets become unreachable.

Vector-based math captures wind-induced velocity adjustments. **Figure 4** portrays wind flowing at an angle during travel between customers. Wind vw impacts the segment from customer $i1$ to $i2$. θw defines the angle formed by the customer vector ($i1$,2) and wind vector vw. vd represents the drone's base flight speed. Computation is needed for the angle linking vd with the customer vector ($i1$,2).

© 2026 The Author(s). | Published by Agro Intelligence Research Press

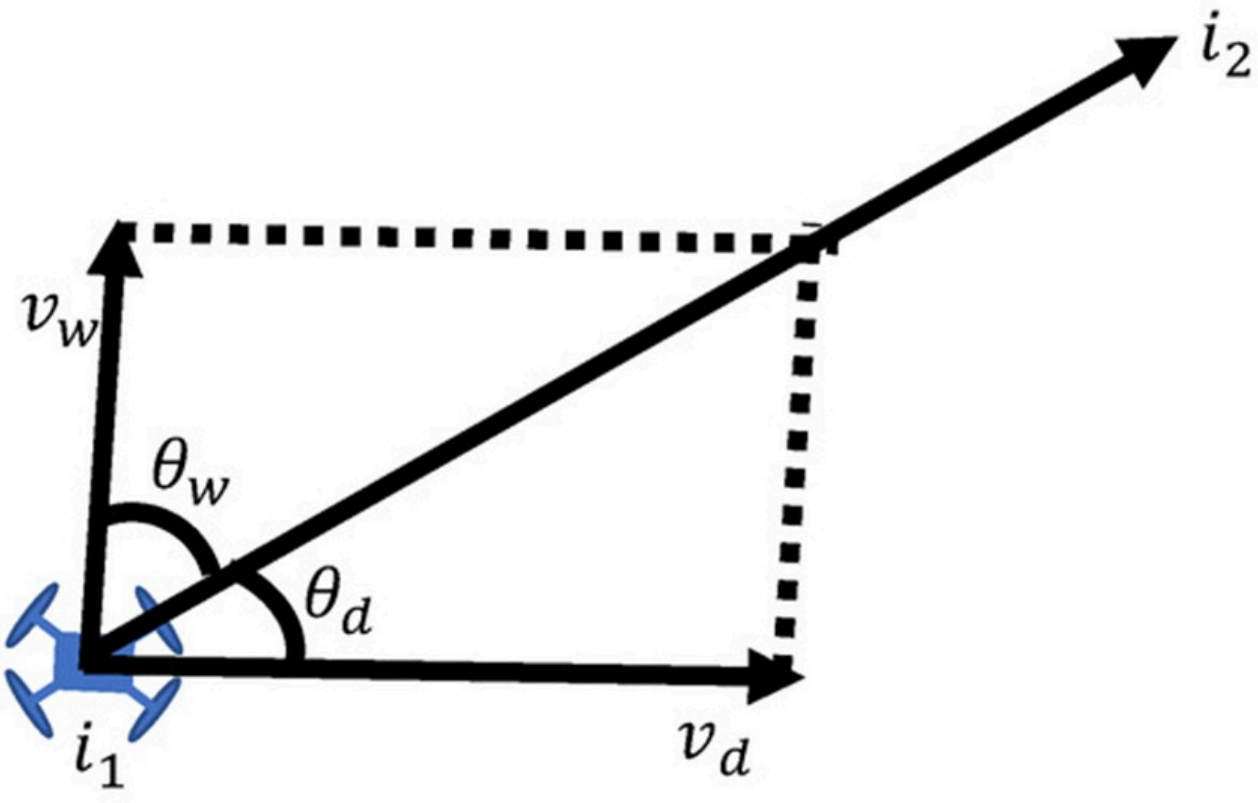


Figure 4. Drone flight under windy conditions.

Figure 5 illustrates velocity modification from wind. v' denotes the resulting drone speed after wind adjustment. For v', the merged vector from drone speed vd plus wind vw must point exactly along the customer vector (i1,2). Given angle θd between vd and (i1,2), $|vd|\sin(\theta d)$ satisfies:

$$|v_d| \sin(\theta_d) = |v_w| \sin(\theta_w) \quad (17)$$

© 2026 The Author(s). | Published by Agro Intelligence Research Press

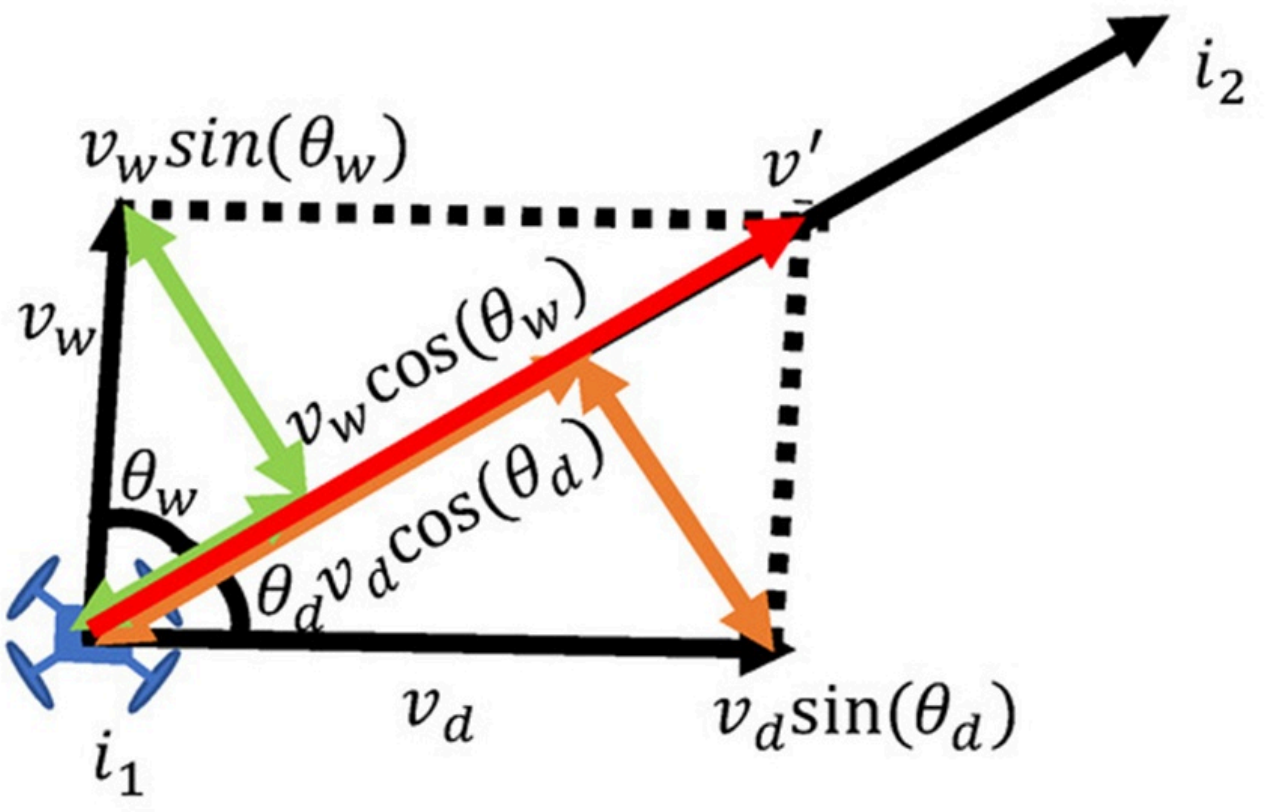


Figure 5. Speed is changed by wind.

Therefore, θd is derived as follows.

$$\theta_d = \arcsin\left(\frac{|v_w|\ \sin\ (\theta_w)}{|v_d|}\right) \quad (18)$$

The norm of the synthetic vector v' of vw and vd can be expressed as follows.

$$|v'| = |v'|\ \cos\ \theta_w + |v_d|\ \cos\ \theta_d \quad (19)$$

According to **Eqs. 18 and 19**, the scalar of vector v' is described in the following formula:

$$\left|v'\right| = |v_w|\ \cos\ (\theta_w) + |v_d|\ \cos\left(\ \arcsin\left(\frac{|v_w|\ \sin\ (\theta_w)}{|v_d|}\right)\right) \quad (20)$$

Where speed vlw of the drone is equal to the scalar value of vector v'.

A Dynamic Programming Algorithm

© 2026 The Author(s). | Published by Agro Intelligence Research Press

We now describe a fast computational procedure for solving the previously defined FSVRPLW. Since FSVRPLW is based on TSP foundations, it is NP-hard. A complete enumeration approach would require ($N!$) operations, making sizable cases infeasible within reasonable limits. Accordingly, this paper offers a dynamic programming procedure for FSVRPLW [33]. Dynamic programming breaks complex tasks into overlapping subtasks and assembles their best solutions into an overall optimal solution. Its strength lies in storing and reusing solutions to identical sub-tasks.

$\mathbb{S}$ represents the collection of visited customers, with i as the most recent one inside $\mathbb{S}$. The pair ($\mathbb{S}$,) forms a state. The base state equals ({0},0). Minimum accumulated flight duration reaching state ($\mathbb{S}$,) from the base is written as ($\mathbb{S}$,). The recurrence relation for determining values of ($\mathbb{S}$,) is given next.

$$T(\mathbb{S}, i) = \min \{ T(\mathbb{S} \setminus i, i') + t(x(i'), x(i)) \mid i' \in \mathbb{S} \setminus i \} \quad (21)$$

Further explanation of this relation follows. With i as the ending customer in $\mathbb{S}$ and i' as the one before it, ($\mathbb{S} \setminus i,'$) stores the least duration from depot up to i'. Meanwhile, ((i'),(i)) gives the duration for the segment from i' to i, incorporating current package mass and wind. The base state ({0},0) holds zero duration before leaving the depot, expressed by:

$$T(\{0\}, 0) = 0 \quad (22)$$

Routing requires the circuit with the lowest total duration that departs the depot, covers every customer exactly once, and returns to the depot. For N customers, this is stated formally as:

$$T(\{0, 1, 2, \ldots, N, 0\}, 0) \quad (23)$$

Eq. 23 decomposes recursively through **Eq. 21**. When sub-problems reach the base case in **Eq. 22**, the minimal-duration route emerges.

Algorithm 1 presents the dynamic programming pseudo-code. *Wall* equals total payload mass while $\mathbb{C}$ lists all customers. *Visited* tracks already-served customers. Algorithm inputs consist of customer quantity, individual package masses, location coordinates, and wind velocity. The output provides the route with the minimum total flight duration. *Visited* is an N-length bit vector, setting the (i−1)-th bit upon visiting customer i. For instance, with 4 customers and customer 2 visited, the vector reads {0010} in binary. [*Visited*][*Customer*] is a matrix holding duration values that correspond to ($\mathbb{S}$,). Thus, Refs. [3] and [6] signals that customers 2 and 3 have been visited, with the current position at customer 3.

Line 1 sums all input payloads into *Wall*. Lines 3–6 determine depot-to-customer durations and record them in *FT*. The *Payload* array logs carried mass at each stage because velocity responds to both load and wind. Lines 8–20 compute durations involving leftover customers. Lines 23–25 handle the return leg duration and record the best overall duration in *MINTIME*. The critical efficiency section spans lines 8–20 and uses triple-nested loops rather than recursion. Computational order equals O(2^N×N^2), considerably quicker than the ($N!$) cost of exhaustive enumeration.

© 2026 The Author(s). | Published by Agro Intelligence Research Press

Input: N: Number of customers, W: Payload of each customer, C: Coordinates of each customer, *Vw*: Wind Vector
Output: Optimal Route: The route that minimizes the total flight time

$Wall \leftarrow \sum W$

for $Next \in \mathbb{C}$ **do**
  $FT[1<<(Next-1)][Next] \leftarrow FlightTime(depottoNext)$
  $Payload[1<<(Next-1)] \leftarrow (Wall-WNext)$
end for

for $Visited \in [0,1,2,\ldots,(2^N-1)]$ **do**
  for $Next \in \mathbb{C}$ **do**
    if $Nexthasnotalreadyvisited$ **then**
      for $Previous \in \mathbb{C}$ **do**
        if $Previoushasbeenalreadyvisited$ **then**
          $FT[Visited|(1<<(Next-1))][Next] \leftarrow min(FT[Visited][Previous]+$
          $FlightTime(PrevioustoNext), FT[Visited|(1<<(Next-1))][Next])$
          $Payload[Visited|(1<<(Next-1))] \leftarrow Payload[Visited]-WNext$
        end if
      end for
    end if
  end for
end for

$MIN_TIME \leftarrow INFINITE$
for $Previous \in \mathbb{C}$ **do**
  $MIN_TIME \leftarrow min(FT[2^N-1][Previous]+FlightTime(Previoustodepot), MIN_TIME)$
end for

Algorithm 1. Dynamic Programming Algorithm for FSVRPLW.

© 2026 The Author(s). | Published by Agro Intelligence Research Press

Evaluation

Experiments test how well the suggested FSVRPLW performs. Multiple routing procedures were coded in Python and benchmarked based on aggregate flight distance, aggregate flight duration, and processing time.

Experimental setup

The comparison involves five routing procedures listed here:

· DPTSP: Dynamic programming procedure for TSP. Determines the route minimizing flight duration. Disregards wind and load.

· DPFS-L: Dynamic programming procedure for FSVRP [11]. Determines the route minimizing flight duration. Accounts solely for load.

· DPFS-W: Dynamic programming procedure for FSVRPLW. Determines the route minimizing flight duration. Accounts solely for wind.

· BFFS-LW: Exhaustive search procedure for FSVRPLW. Evaluates every possible route (N! total) seeking minimal durations.

· DPFS-LW: The dynamic programming procedure introduced in Section 4 for FSVRPLW. This constitutes the suggested technique.

Customer quantities ranged between 5 and 20. Twenty distinct random instances were generated per quantity, differing in customer positions, package masses, wind bearings, and wind velocities. Overall, this yielded 320 instances. Assessments examined flight duration, flight distance, and procedure runtime. The AR. Drone 2.0 served as a reference model for calculations. Prior experience within our group on the AR. Drone 2.0 supported accurate parameter choices. Importantly, the technique applies independently of the drone model. Base velocity without payload equals 5 m/s. Drone mass equals 490 g. Payload limit is 200 g, restricting the combined carried mass to 200 g. Constant wind velocity equals 2 m/s. This setting ensured continued flight capability even at peak payload. Although the AR. The drone model is used as a reference; the framework accommodates other drones, including larger variants for heavier cargo. Initial testing verified AR. Drone capability below 200 g. Loads under 200 g suit items like papers and correspondence. Computation time was restricted to 3600 s.

Experimental results

Figure 6 exhibits flight duration outcomes across the five procedures. The vertical scale presents each procedure's duration normalized relative to DPFS-LW. Since there are 20 instances per customer quantity, the bars reflect the mean values. The horizontal scale indicates customer quantities. BFFS-LW matches DPFS-LW exactly up through 11 customers, verifying that both locate optimal answers. Results for BFFS-LW cease after 12 customers because processing exceeds 1 hour. The suggested DPFS-LW consistently delivers the lowest durations. Relative to DPFS-L, DPFS-LW lowered flight duration by 5.10% on average. Compared with DPTSP, DPFS-LW reduced it by 18.46% on average. The mean gap between DPTSP and DPFS-W is 1.98%. The mean gap between DPTSP and DPFS-L is 13.35%. This separation exceeds corresponding differences in flight distance. Hence, wind exerts a noticeable influence on duration. Although DPTSP omits both load and wind, it never recorded the highest durations in any case. The presence of several equally viable solutions prevents DPTSP from always showing the worst performance.

© 2026 The Author(s). | Published by Agro Intelligence Research Press

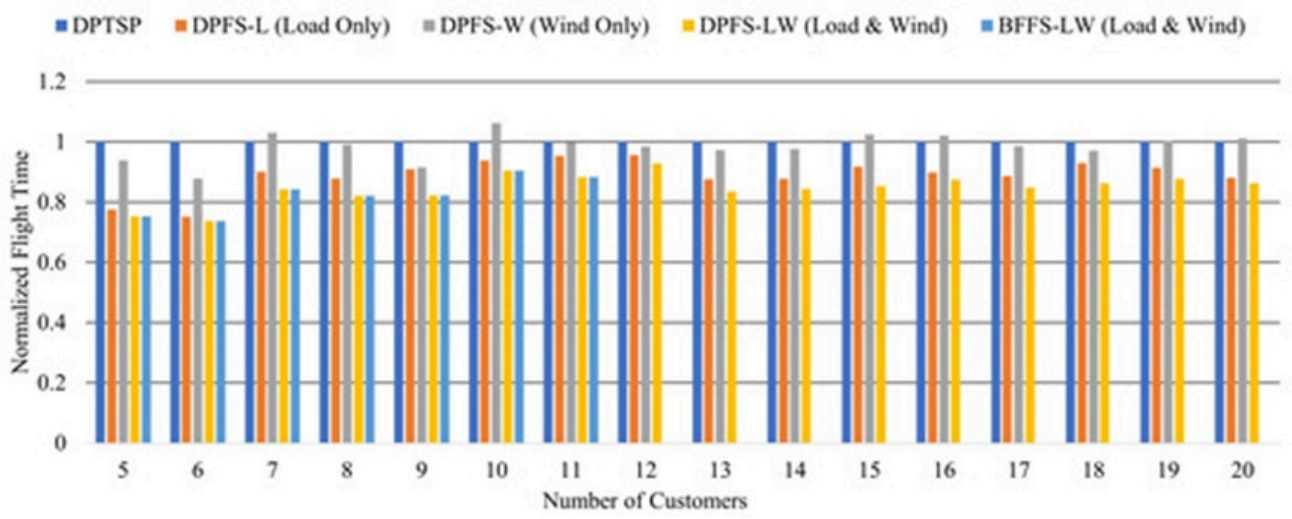


Figure 6. Comparison of flight time.

Next, **Figure 7** shows the result of the five methods in terms of flight distance. The vertical axis shows the flight distance for each method, normalized by DPFS-LW. The horizontal axis shows the number of customers. BFFS-LW and DPFS-LW show the same results until the number of customers is 11. This shows that both the brute-force and dynamic programming algorithms can find the solution. The results of BFFS-LW are not shown because the calculation time exceeds 1 hour for more than 12 customers. The proposed method, DPFS-LW, has the longest flight distance in all results. Comparing DPFS-L and DPFS-LW, the flight distance of DPFS-LW increased by 1.43% on average. It is believed that the flight distance increases when wind is used during flight compared to the prior method. DPTSP has the shortest flight distance in all results. Comparing DPTSP and DPFS-LW, the flight distance of DPTSP is shorter by 2.42% on average. The flight distances of DPTSP and DPFS-W are very close to each other. The average difference between DPTSP and DPFS-W is 0.18%. On the other hand, the average difference between DPTSP and DPFS-L is 1.00%. This indicates that the wind does not have a significant effect on flight distance.

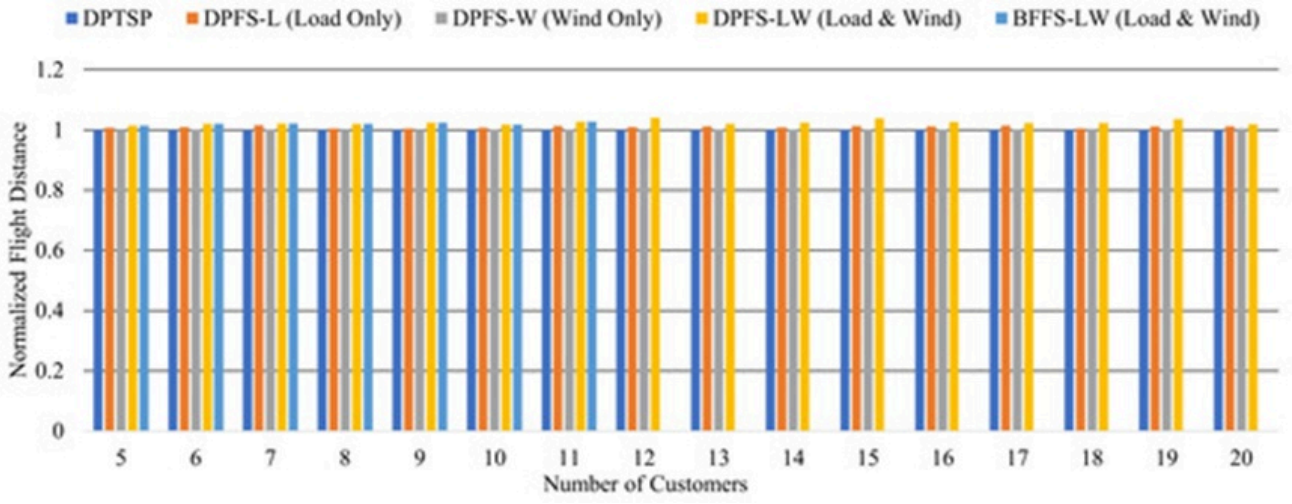


Figure 7. Comparison of flight distance.

The outcomes reveal that the suggested DPFS-LW lengthens flight distance yet shortens flight time. This stems from exploiting wind and load factors, enabling more efficient package transport. These findings highlight the importance of accounting for speed adjustments due to payload and wind during drone operations.

© 2026 The Author(s). | Published by Agro Intelligence Research Press

In this paper, the wind is assumed to be constant in direction and speed, but it dynamically changes. In this paper, we simplify the wind model to evaluate how flight time changes with wind. Undoubtedly, the drone's response to wind can change for various reasons. Therefore, it is necessary to verify the effect of wind on the drone in more detail, which is considered in one of our future works.

Next, **Figure 8** shows the runtime of each method by using a logarithmic scale. The vertical axis shows runtime, and the horizontal axis shows the number of customers. The methods mentioned, except for BFFS-LW, can find a solution within 1 hour. This result shows that our proposed algorithm remains useful even with 20 customers.

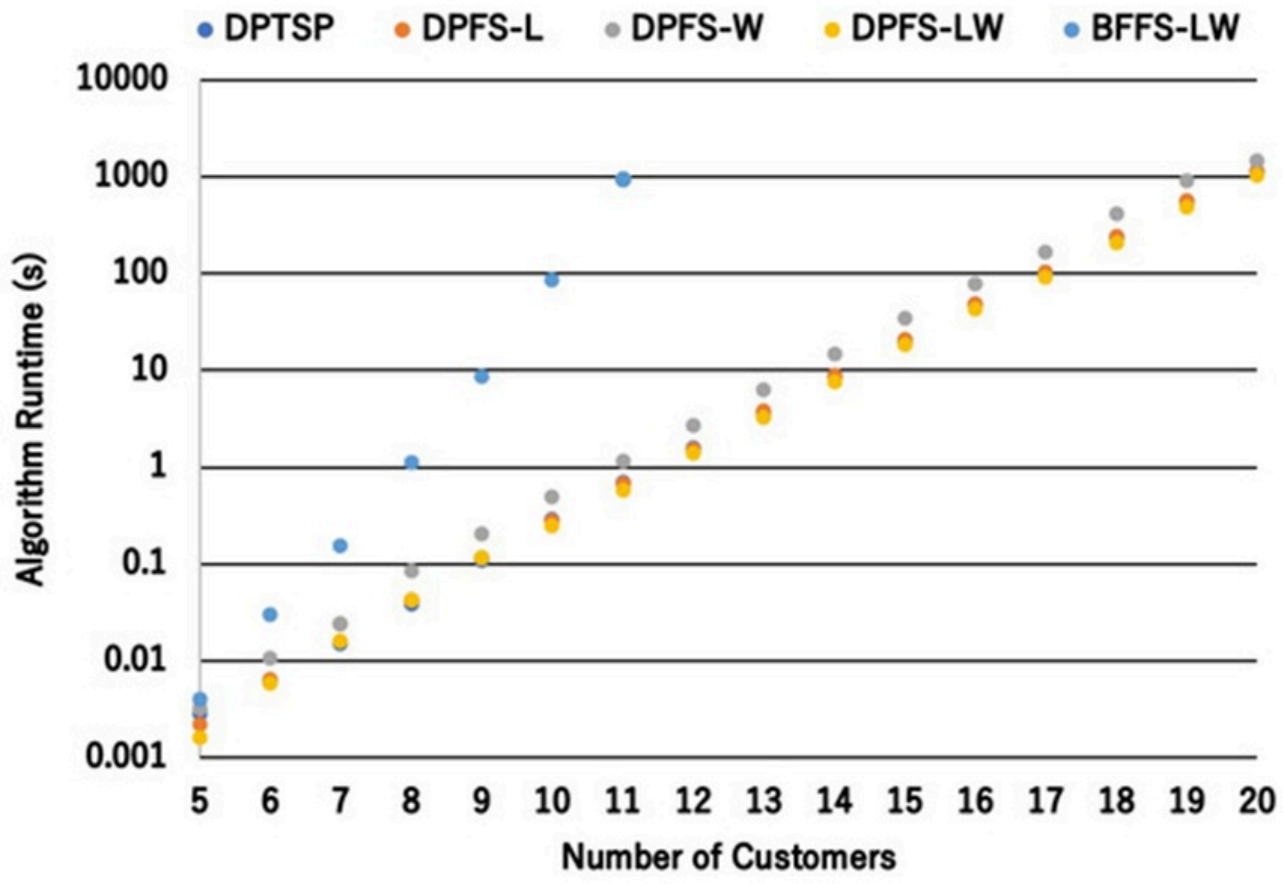


Figure 8. Algorithm runtime.

Conclusion

Drones are expected to become popular delivery vehicles. In this paper, we formulated FSVRPLW, which is an extension of FSVRP. The problem determines an optimal route that minimizes the total flight time, accounting for the drone's load weight and wind effects on its flight speed. To effectively solve the problem, we also proposed a dynamic programming algorithm. Experimental results show the effectiveness of the proposed algorithm. In future work, we will consider dynamic changes in wind conditions and the division of packages across multiple tours.

Acknowledgements

None

© 2026 The Author(s). | Published by Agro Intelligence Research Press

Conflict of interest

None

Financial support

This work is in part supported by KAKENHI 20H04160 and 20J21208.

Ethics statement

None

Received: 22 Oct 2024 Revised: 27 Dec 2024 Accepted: 13 Jan 2025
Published online: 25 November 2026

Rights and permissions

Open Access The author(s) retain copyright. This article is licensed under the Creative Commons Attribution-NonCommercial-ShareAlike 4.0 International License. It may be shared and adapted for non-commercial purposes with appropriate attribution, an indication of changes, and distribution of adaptations under the same license. Third-party material may be subject to separate terms identified in its credit line. View the license at https://creativecommons.org/licenses/by-nc-sa/4.0/.

References

1. Kirschstein T. Comparison of energy demands of drone-based and ground-based parcel delivery services. Transp Res Part D Transp Environ. 2020;78:102209.

2. Amazon Prime Air. www.amazon.com/b?node=8037720011 (accessed on 22 October 2021).

3. Project Wing. https://x.company/projects/wing/ (accessed on 22 October 2021).

4. Viloria DR, Solano-Charris EL, Muñoz-Villamizar A, Montoya-Torres JR. Unmanned aerial vehicles/drones in vehicle routing problems: A literature review. Int Trans Oper Res. 2021;28:1626–57.

5. Macrina G, Pugliese LDP, Guerriero F, Laporte G. Drone-aided routing: A literature review. Transp Res Part C Emerg Technol. 2020;120:102762.

6. Chung SH, Sah B, Lee J. Optimization for drone and drone-truck combined operations: A review of the state of the art and future directions. Comput Oper Res. 2020;123:105004.

7. Khoufi I, Laouiti A, Adjih C. A survey of recent extended variants of the traveling salesman and vehicle routing problems for unmanned aerial vehicles. Drones. 2019;3:66.

8. Applegate DL, Bixby RE, Chvátal V, Cook WJ. The traveling salesman problem. Princeton, NJ, USA: Princeton University Press; 2011.

9. Dorling K, Heinrichs J, Messier GG, Magierowski S. Vehicle routing problems for drone delivery. IEEE Trans Syst Man Cybern Syst. 2016;47:70–85.

10. Ito S, Negoro S, Kong X, Taniguchi I, Tomiyama H. A methodology for measuring flight speed of drones in indoor environments. Procedia Comput Sci. 2021;187:322–8.

11. Funabashi Y, Taniguchi I, Tomiyama H. Work-in-progress: Routing of delivery drones with load-dependent flight speed. In: Proceedings of the 2019 IEEE Real-Time Systems Symposium (RTSS); Hong Kong, China; 2019. p. 520–3.

12. Ito S, Nishikawa H, Kong X, Funabashi Y, Shibata A, Negoro S, et al. Energy-aware routing of delivery drones under windy conditions. IPSJ Trans Syst Lsi Des Methodol. 2021;14:30–9.

13. Luo H, Liang Z, Zhu M, Hu X, Wang G. Integrated optimization of unmanned aerial vehicle task allocation and path planning under steady wind. PLoS ONE. 2018;13:e0194690.

14. Guerrero JA, Bestaoui Y. UAV path planning for structure inspection in windy environments. J Intell Robot Syst. 2013;69:297–311.

15. Zhang J, Campbell JF, Sweeney DC II, Hupman AC. Energy consumption models for delivery drones: A comparison and assessment. Transp Res Part D Transp Environ. 2021;90:102668.

16. Agatz N, Bouman P, Schmidt M. Optimization approaches for the traveling salesman problem with drone. Transp Sci. 2018;52:965–81.

17. Bouman P, Agatz N, Schmidt M. Dynamic programming approaches for the traveling salesman problem with drone. Networks. 2018;72:528–42.

18. Marinelli M, Caggiani L, Ottomanelli M, Dell'Orco M. En route truck–drone parcel delivery for optimal vehicle routing strategies. IET Intell Transp Syst. 2018;12:253–61.

19. Ha QM, Deville Y, Pham QD, Hoàng Hà M. On the min-cost traveling salesman problem with drone. Transp Res Part C Emerg Technol. 2018;86:597–621.

20. Murray CC, Chu AG. The flying sidekick traveling salesman problem: Optimization of drone-assisted parcel delivery. Transp Res Part C Emerg Technol. 2015;54:86–109.

21. Tu PA, Dat NT, Dung PQ. Traveling salesman problem with multiple drones. In: Proceedings of the Ninth International Symposium on Information and Communication Technology; Danang City, Vietnam; 2018. p. 46–53.

22. Kitjacharoenchai P, Ventresca M, Moshref-Javadi M, Lee S, Tanchoco JMA, Brunese PA. Multiple traveling salesman problem with drones: Mathematical model and heuristic approach. Comput Ind Eng. 2019;129:14–30.

23. Saleu RM, Deroussi L, Feillet D, Grangeon N, Quilliot A. An iterative two-step heuristic for the parallel drone scheduling traveling salesman problem. Networks. 2018;72:459–74.

24. Ham AM. Integrated scheduling of M-truck, M-drone, and M-depot constrained by time-window, drop-pickup, and M-visit using constraint programming. Transp Res Part C Emerg Technol. 2018;91:1–14.

25. Poikonen S, Wang X, Golden B. The vehicle routing problem with drones: Extended models and connections. Networks. 2017;70:34–43.

26. Wang Z, Sheu JB. Vehicle routing problem with drones. Transp Res Part B Methodol. 2019;122:350–64.

27. Ha QM, Deville Y, Pham QD, Hoàng Hà M. A hybrid genetic algorithm for the traveling salesman problem with drone. J Heuristics. 2020;26:219–47.

© 2026 The Author(s). | Published by Agro Intelligence Research Press

28. Kara I, Kara BY, Yetis MK. Energy minimizing vehicle routing problem. In: Proceedings of the International Conference on Combinatorial Optimization and Applications; Xi'an, China; 2007. p. 62–71.

29. Funabashi Y, Shibata A, Negoro S, Taniguchi I, Tomiyama H. A dynamic programming algorithm for energy-aware routing of delivery drones. In: Advances in Artificial Intelligence and Data Engineering; Springer: Singapore; 2021. p. 1217–26.

30. Ito S, Negoro S, Kong X, Taniguchi I, Tomiyama H. Improved modeling of energy consumption of delivery drones. In: Proceedings of the Workshop on Synthesis and System Integration of Mixed Information Technologies (SASIMI); Online; 2021. p. 56–60.

31. Shivgan R, Dong Z. Energy-efficient drone coverage path planning using genetic algorithm. In: Proceedings of the IEEE International Conference on High Performance Switching and Routing (HPSR); Newark, NJ, USA; 2020. p. 1–6.

32. Peng K, Du J, Lu F, Sun Q, Dong Y, Zhou P, Hu M. A hybrid genetic algorithm on routing and scheduling for vehicle-assisted multi-drone parcel delivery. IEEE Access. 2019;7:49191–9200.

33. Held M, Karp RM. A dynamic programming approach to sequencing problems. J Soc Ind Appl Math. 1962;10:196–210.

© 2026 The Author(s). | Published by Agro Intelligence Research Press